Supplement of Earth Syst. Dynam., 16, 1833–1844, 2025
https://doi.org/10.5194/esd-16-1833-2025-supplement

Earth System Dynamics
Open Access
EGU

Supplement of

Causal mechanisms of subpolar gyre variability in CMIP6 models

Swinda K. J. Falkena et al.

Correspondence to: Swinda K. J. Falkena (s.k.j.falkena@uu.nl)

S1. Model Details

Table S1: The models used in this study, with the length of the dataset (in years), whether the barotropic streamfunction is available and the relevant references

Model	Length	msftbarot	Reference
ACCESS-CM2	500	X	Dix et al. (2019)
ACCESS-ESM1-5	900		Ziehn et al. (2019)
BCC-CSM2-MR	600	X	Wu et al. (2018)
BCC-ESM1	165	X	Zhang et al. (2018)
CAS-ESM2-0	549		Chai (2020)
CESM2-FV2	500	X	Danabasoglu (2019a)
CESM2-WACCM-FV2	500	X	Danabasoglu (2019b)
CESM2-WACCM	499	X	Danabasoglu (2019c)
CESM2	1200	X	Danabasoglu et al. (2019)
CMCC-CM2-SR5	500	X	Lovato and Peano (2020)
CMCC-ESM2	250	X	Lovato et al. (2021)
CNRM-CM6-1-HR	300		Voldoire (2019)
CNRM-CM6-1	500		Voldoire (2018)
CNRM-ESM2-1	500		Seferian (2018)
CanESM5-1	501	X	Swart et al. (2019b)
CanESM5	1000	X	Swart et al. (2019a)
E3SM-1-0	500		Bader et al. (2018)
E3SM-1-1-ECA	165		Bader et al. (2019)
E3SM-1-1	165		Bader et al. (2019)
E3SM-2-0-NARRM	500		Bader et al. (2022)
E3SM-2-0	500		Bader et al. (2022)
EC-Earth3-AerChem	311	X	EC-Earth Consortium (EC-Earth) (2020a)
EC-Earth3-CC	505	X	EC-Earth Consortium (EC-Earth) (2021)
EC-Earth3-LR	201		EC-Earth Consortium (EC-Earth) (2019c)
EC-Earth3-Veg-LR	501	X	EC-Earth Consortium (EC-Earth) (2020b)
EC-Earth3-Veg	500	X	EC-Earth Consortium (EC-Earth) (2019a)
EC-Earth3	501	X	EC-Earth Consortium (EC-Earth) (2019b)
FGOALS-f3-L	500	X	Yu (2019)
FGOALS-g3	700	X	Li (2019)
GFDL-ESM4	500		Krasting et al. (2018)
GISS-E2-1-G	851	X	NASA Goddard Institute for Space Studies (NASA/GISS) (2018)
GISS-E2-2-G	151	X	NASA Goddard Institute for Space Studies (NASA/GISS) (2019)
HadGEM3-GC31-LL	500	X	Ridley et al. (2018)
HadGEM3-GC31-MM	500	X	Ridley et al. (2019)
ICON-ESM-LR	500		Lorenz et al. (2021)
IPSL-CM6A-LR	500	X	Boucher et al. (2018)
IPSL-CM6A-MR1	500		Boucher et al. (2023)
KIOST-ESM	500		Kim et al. (2019)
MIROC6	800	X	Tatebe and Watanabe (2018)
MPI-ESM-1-2-HAM	780	X	Neubauer et al. (2019)
MPI-ESM1-2-HR	500	X	Jungclaus et al. (2019)
MPI-ESM1-2-LR	1000	X	Wieners et al. (2019)
MRI-ESM2-0	701	X	Yukimoto et al. (2019)
NESM3	500		Cao and Wang (2019)
NorCPM1	500		Bethke et al. (2019)
NorESM2-LM	501	X	Seland et al. (2019)
NorESM2-MM	500	X	Bentsen et al. (2019)
UKESM1-0-LL	1100	X	Tang et al. (2019)
UKESM1-1-LL	107	X	Mulcahy et al. (2022)

S2. Convection Mechanisms

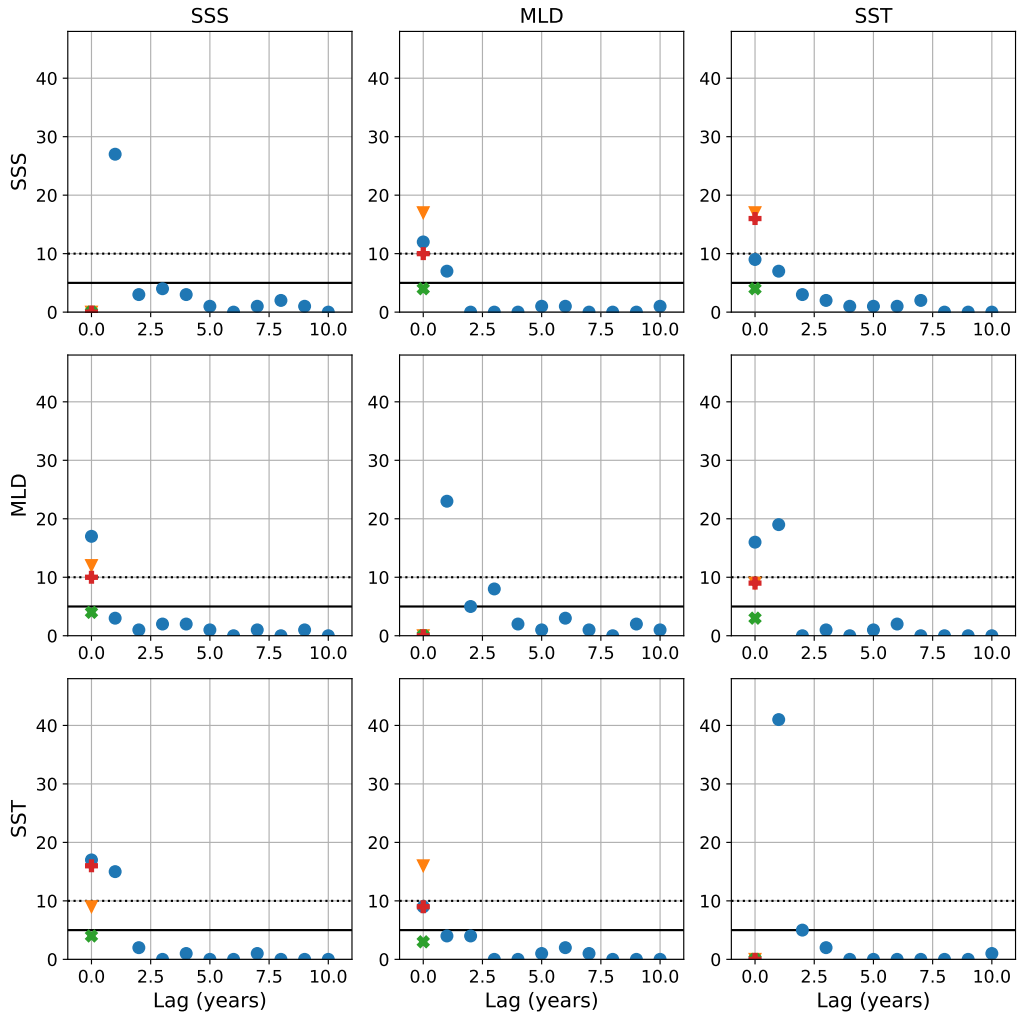

Figure S1: The number of models (out of 47) for which a significant link is found (at the 5%-level) for lags of up to 10 years. Blue circles indicate the number of rightward links following, i.e. from the row to the column variable. For contemporaneous links orange triangles show links directed in leftward and both green crosses and red plusses are links for which the direction could not be determined, either because the orientation rules could not be applied or because they conflicted, respectively.

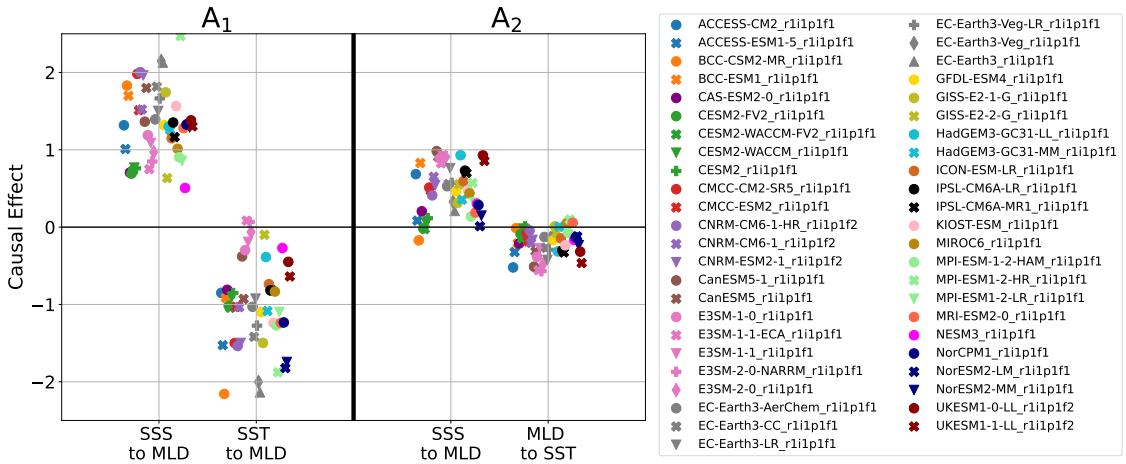

Figure S2: The causal effect for each of the convection mechanisms links for all considered CMIP6 models.

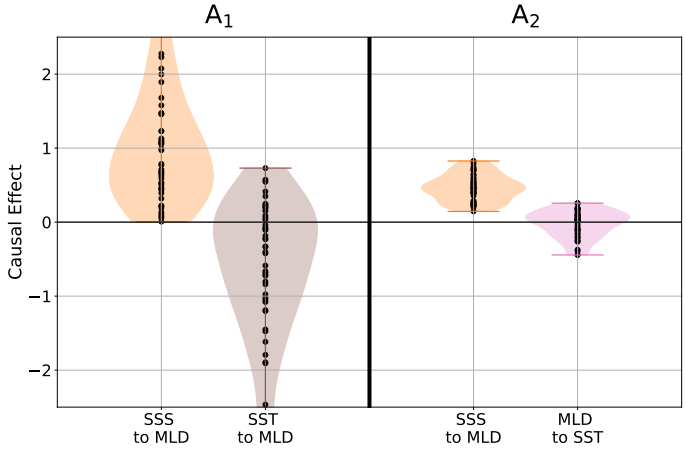

Figure S3: As Figure 3, but using the Labrador sea box to compute the variables.

S3. Subpolar Gyre Variability Mechanism

Table S2: The models for which a link between two variables is found to be significant at the 5%-level.

Link	Lag	Significant Models
SPG→SSS	1	ACCESS-CM2, CESM2-FV2, CESM2-WACCM, CESM2, FGOALS-g3, GISS-E2-1-G, GISS-E2-2-G, HadGEM3-GC31-LL
SSS→MLD	0	ACCESS-CM2, CESM2-WACCM-FV2, CESM2, CMCC-CM2-SR5, CMCC-ESM2, CanESM5, EC-Earth3-CC, EC-Earth3-Veg-LR, FGOALS-f3-L, GISS-E2-1-G, HadGEM3-GC31-LL, HadGEM3-GC31-MM, MPI-ESM-1-2-HAM, MPI-ESM1-2-LR, MRI-ESM2-0, NorESM2-LM, NorESM2-MM, UKESM1-1-LL
	1	BCC-CSM2-MR, BCC-ESM1, CESM2-WACCM, CMCC-CM2-SR5, CMCC-ESM2, CanESM5, EC-Earth3-CC, MIROC6, MPI-ESM1-2-LR, MRI-ESM2-0, UKESM1-0-LL
MLD→SubT	0	ACCESS-CM2, BCC-ESM1, CESM2-FV2, CESM2-WACCM-FV2, CESM2, CMCC-CM2-SR5, EC-Earth3-AerChem, EC-Earth3, FGOALS-f3-L, FGOALS-g3, GISS-E2-1-G, GISS-E2-2-G, HadGEM3-GC31-LL, HadGEM3-GC31-MM, IPSL-CM6A-LR, MIROC6, MPI-ESM-1-2-HAM, MPI-ESM1-2-HR, MRI-ESM2-0, NorESM2-LM, NorESM2-MM, UKESM1-0-LL
	1	CMCC-ESM2, CanESM5, EC-Earth3-CC, EC-Earth3-Veg-LR, EC-Earth3-Veg, IPSL-CM6A-LR, NorESM2-MM
SubT→Rho	0	BCC-ESM1, CESM2-FV2, GISS-E2-2-G, HadGEM3-GC31-MM, MPI-ESM1-2-HR, NorESM2-LM, UKESM1-0-LL
	1	CESM2-FV2, CESM2-WACCM, CESM2, CMCC-CM2-SR5, NorESM2-LM, NorESM2-MM
Rho→SPG	0	EC-Earth3-AerChem, EC-Earth3, GISS-E2-1-G, GISS-E2-2-G, MPI-ESM1-2-HR, MPI-ESM1-2-LR, UKESM1-0-LL
	1	BCC-CSM2-MR, CESM2-WACCM, CESM2, CMCC-CM2-SR5, CMCC-ESM2, EC-Earth3-CC, FGOALS-f3-L, GISS-E2-1-G, MIROC6, MRI-ESM2-0, NorESM2-LM

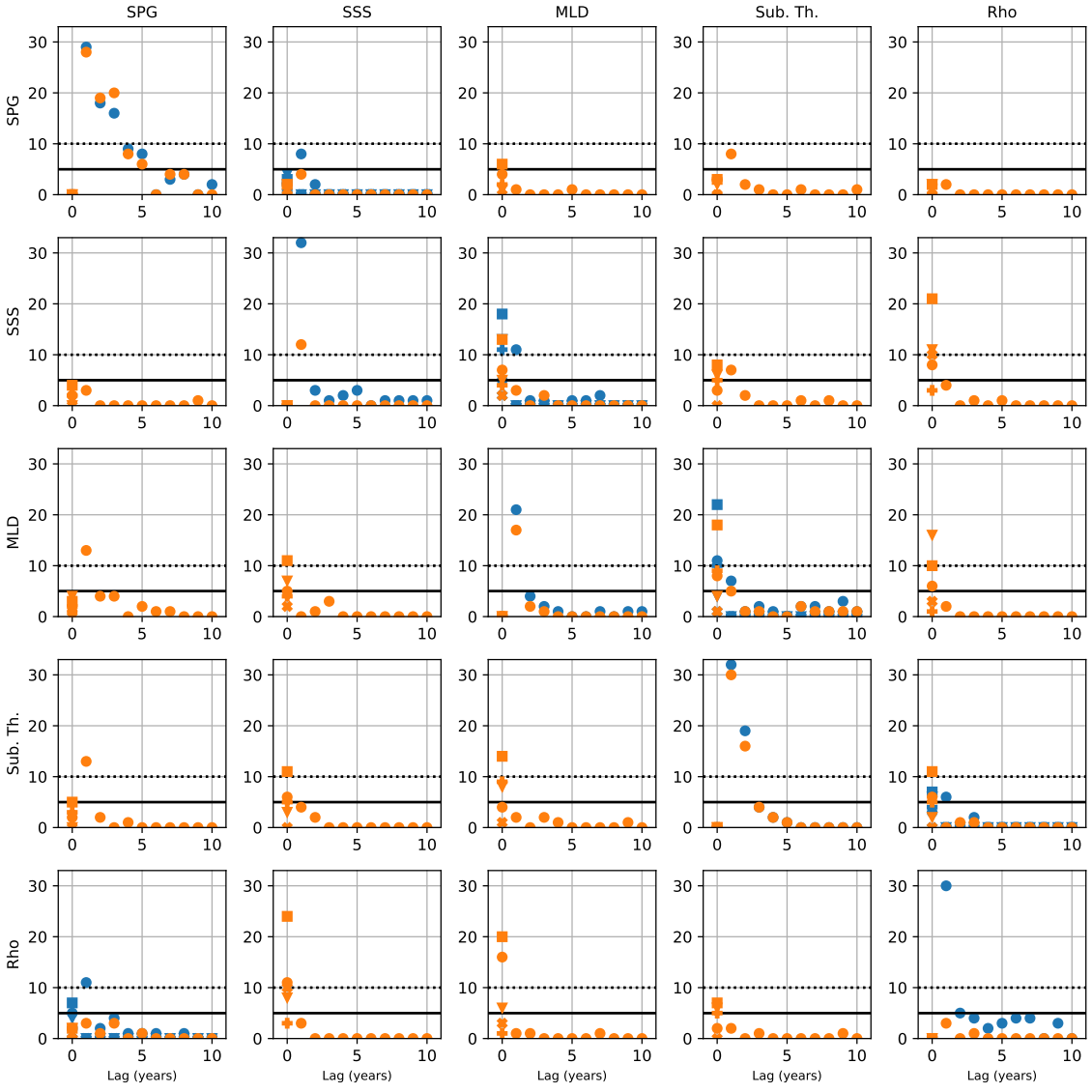

Figure S4: The number of models for which a significant link is found. In orange results including all 5 variables at once are shown as a robustness check, where in blue the results following the theoretical network are given (i.e. including the two variables of a link X→Y and the parent Z of X (Z→X). For direct links there are different markers (as in Figure 4), with the squares giving the sum of the right, undirected and unclear links.

Table S3: The models for which a link from a variable to itself is found to be significant at the 5%-level.

Link	Lag	Significant Models
SPG	1	ACCESS-CM2, BCC-CSM2-MR, BCC-ESM11, CESM2-FV2, CESM2-WACCM, CESM2, CMCC-CM2-SR5, CMCC-ESM2, CanESM5-1, CanESM5, EC-Earth3-AerChem, EC-Earth3-CC, EC-Earth3-Veg-LR, EC-Earth3-Veg, EC-Earth3, FGOALS-f3-L, GISS-E2-1-G, GISS-E2-2-G, HadGEM3-GC31-LL, HadGEM3-GC31-MM, IPSL-CM6A-LR, MIROC6, MPI-ESM-1-2-HAM, MPI-ESM1-2-HR, MPI-ESM1-2-LR, MRI-ESM2-0, NorESM2-LM, NorESM2-MM, UKESM1-0-LL
	2	BCC-CSM2-MR, BCC-ESM1, CESM2-FV2, CESM2, CanESM5-1, CanESM5, EC-Earth3-AerChem, EC-Earth3-CC, EC-Earth3-Veg-LR, EC-Earth3-Veg, EC-Earth3, GISS-E2-1-G, HadGEM3-GC31-MM, IPSL-CM6A-LR, MIROC6, MPI-ESM1-2-HR, UKESM1-0-LL
	3	BCC-CSM2-MR, BCC-ESM1, CESM2-FV2, CESM2, CMCC-CM2-SR5, CanESM5-1, CanESM5, EC-Earth3-AerChem, EC-Earth3-Veg-LR, EC-Earth3-Veg, EC-Earth3, FGOALS-f3-L, FGOALS-g3, HadGEM3-GC31-LL, HadGEM3-GC31-MM, IPSL-CM6A-LR, MIROC6, MPI-ESM1-2-HR, MRI-ESM2-0, UKESM1-0-LL
	4	CMCC-ESM2, CanESM5, EC-Earth3-CC, HadGEM3-GC31-MM, IPSL-CM6A-LR, 'MIROC6, MRI-ESM2-0, UKESM1-0-LL
	5	CMCC-CM2-SR5, CanESM5-1, CanESM5, EC-Earth3-Veg, HadGEM3-GC31-LL, 'UKESM1-0-LL
SSS	1	ACCESS-CM2, BCC-CSM2-MR, BCC-ESM1, CESM2-FV2, CESM2-WACCM-FV2, CESM2-WACCM, CESM2, CMCC-CM2-SR5, CMCC-ESM2, CanESM5, FGOALS-g3, 'GISS-E2-1-G, GISS-E2-2-G, HadGEM3-GC31-LL, HadGEM3-GC31-MM, IPSL-CM6A-LR, MIROC6, MPI-ESM-1-2-HAM, MPI-ESM1-2-HR, MPI-ESM1-2-LR, MRI-ESM2-0, NorESM2-LM, NorESM2-MM, UKESM1-0-LL
MLD	1	ACCESS-CM2, BCC-ESM1, CESM2, CMCC-CM2-SR5, CanESM5, EC-Earth3-AerChem, EC-Earth3-CC, EC-Earth3, HadGEM3-GC31-LL, HadGEM3-GC31-MM, IPSL-CM6A-LR, MIROC6, MPI-ESM-1-2-HAM, MPI-ESM1-2-HR, MPI-ESM1-2-LR, MRI-ESM2-0, NorESM2-LM, NorESM2-MM, UKESM1-0-LL
SubT	1	All models
	2	ACCESS-CM2, CMCC-CM2-SR5, CanESM5-1, CanESM5, EC-Earth3-AerChem, EC-Earth3-CC, EC-Earth3-Veg-LR, EC-Earth3-Veg, EC-Earth3, FGOALS-f3-L, HadGEM3-GC31-LL, IPSL-CM6A-LR, MIROC6, MPI-ESM-1-2-HAM, MPI-ESM1-2-HR, MPI-ESM1-2-LR, MRI-ESM2-0, UKESM1-0-LL
Rho	0	ACCESS-CM2, BCC-CSM2-MR, BCC-ESM11, CESM2-FV2, CESM2-WACCM-FV2, CESM2-WACCM, CESM2, CMCC-CM2-SR5, CanESM5-1, CanESM5, EC-Earth3-AerChem, EC-Earth3-CC, EC-Earth3-Veg-LR, EC-Earth3-Veg, EC-Earth3, FGOALS-f3-L, FGOALS-g3, GISS-E2-1-G, GISS-E2-2-G, HadGEM3-GC31-LL, HadGEM3-GC31-MM, IPSL-CM6A-LR, MIROC6, MPI-ESM-1-2-HAM, MPI-ESM1-2-HR, MPI-ESM1-2-LR, MRI-ESM2-0, NorESM2-LM, NorESM2-MM, UKESM1-0-LL, UKESM1-1-LL

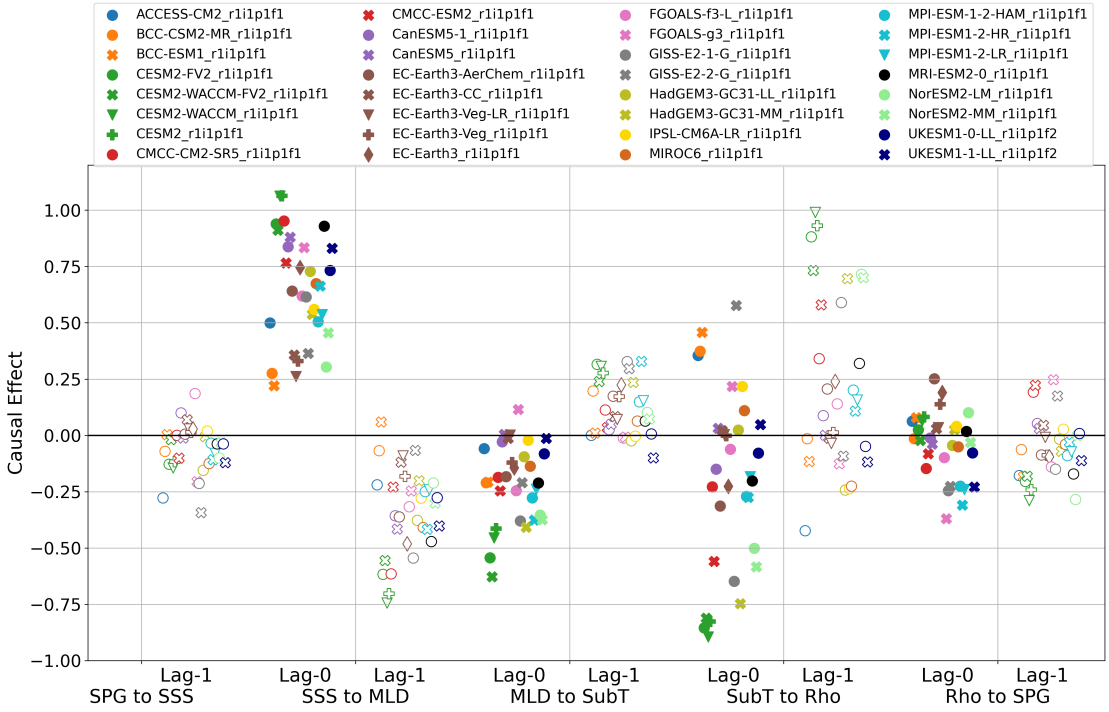

Figure S5: The causal effect for each of the subpolar gyre mechanism links for all considered CMIP6 models. For each link, the solid markers indicate the contemporaneous links and the empty ones the link at lag-1.

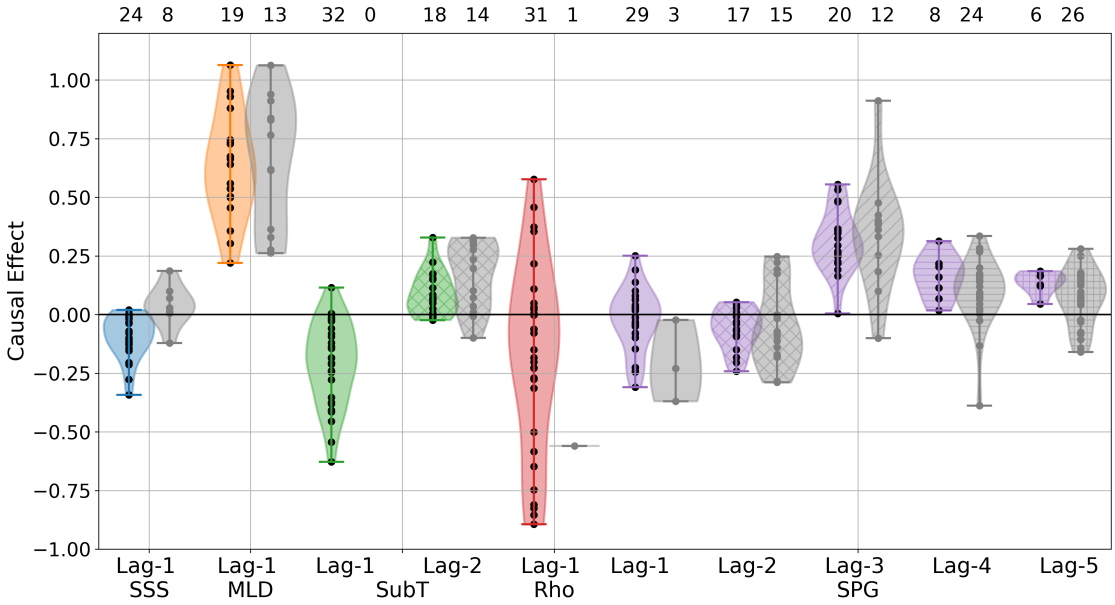

Figure S6: The causal effect for each variable to itself at lags for which at least 5 models indicate a significant effect at the 5% level. The violins in colour give the distribution over the models for which the link is significant, with the black dots indicating the individual model values. The grey violins and grey dots show the non-significant results. Hatching indicates the causal effect at different lags (2 and up). The numbers at the top indicate the number of models for which that link is significant, respectively not significant, at the 5% level.

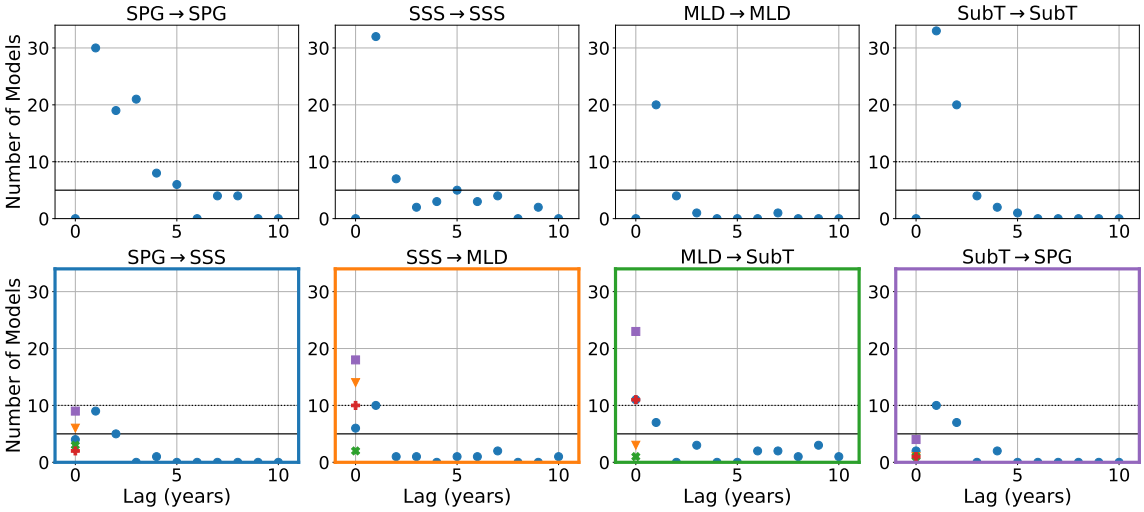

Figure S7: As Figure 4, but without Rho as a variable.

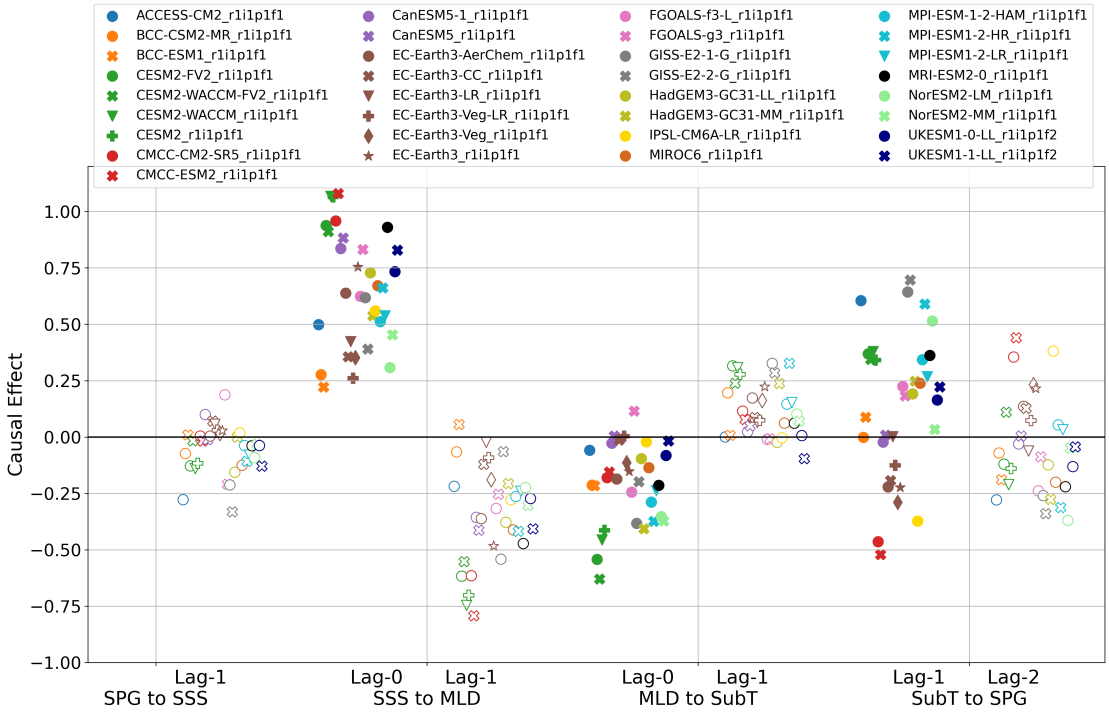

Figure S8: The causal effect for each of the links when omitting Rho for all considered CMIP6 models.

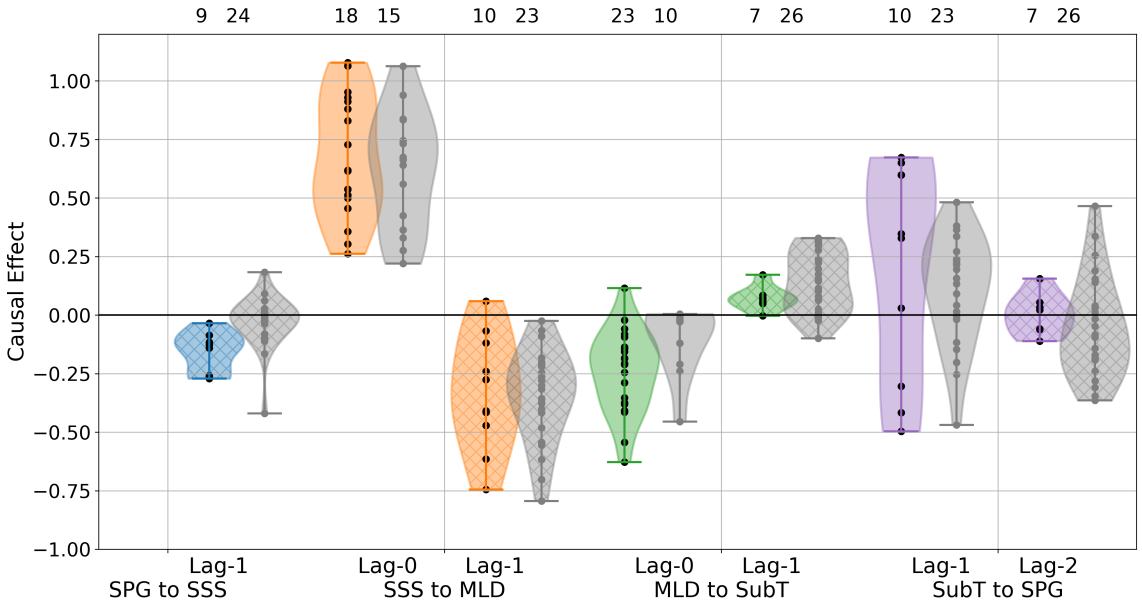

Figure S9: As Figure 5, but without Rho as a variable. As for the main result only links which are significant for at least 5 models at the 5%-level are included. For the SubT→SPG link this is the case for both lag-1 and lag-2. The results for the other links do not change much when omitting Rho. We find the link from SubT to SPG tends towards a positive sign in models where it is significant.

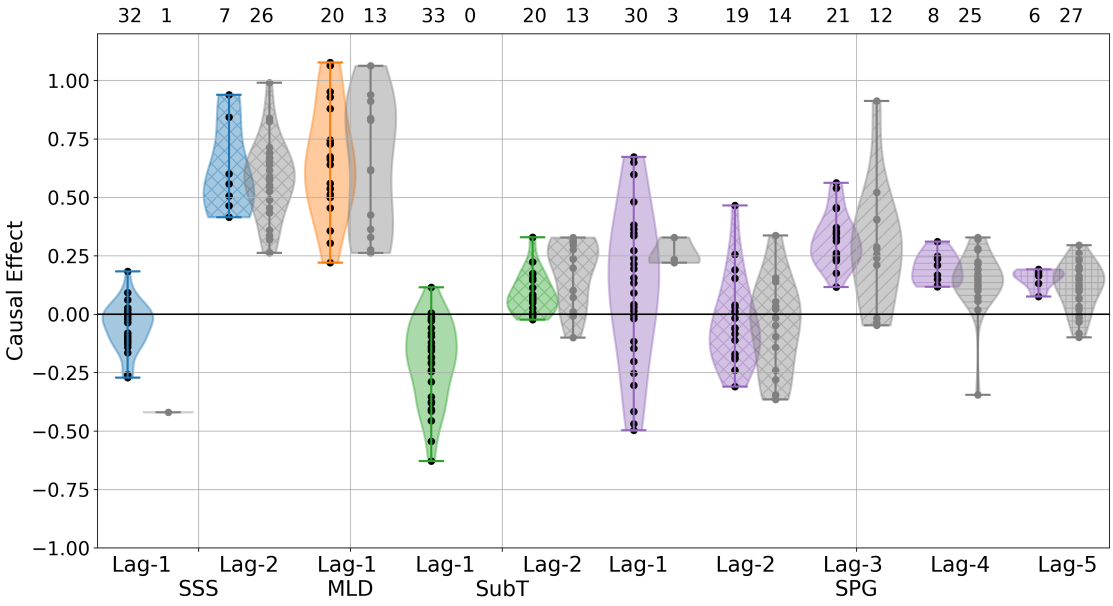

Figure S10: As Figure S6, but without Rho as a variable. As for the main result only links which are significant for at least 5 models at the 5%-level are included.

References

Bader, D., Leung, R., Taylor, M., and McCoy, R.: E3SM-Project E3SM1.0 model output prepared for CMIP6 CMIP piControl, https://doi.org/10.22033/esgf/cmip6.4499, 2018.

Bader, D., Leung, R., Taylor, M., and McCoy, R.: E3SM-Project E3SM1.1 model output prepared for CMIP6 CMIP piControl, https://doi.org/10.22033/esgf/cmip6.11489, 2019.

Bader, D., Leung, R., Taylor, M., and McCoy, R.: E3SM-Project E3SM2.0 model output prepared for CMIP6 CMIP piControl, https://doi.org/10.22033/esgf/cmip6.16970, 2022.

Bentsen, M., Oliviè, D. J. L., Tjiputra, J., Toniazzo, T., Gjermundsen, A., Graff, L. S., Debernard, J. B., Gupta, A. K., He, Y., Kirkevåg, A., Schwinger, J., Tjiputra, J., Aas, K. S., Bethke, I., Fan, Y., Griesfeller, J., Grini, A., Guo, C., Ilicak, M., Karset, I. H. H., Landgren, O. A., Liakka, J., Moseid, K. O., Nummelin, A., Spensberger, C., Tang, H., Zhang, Z., Heinze, C., Iversen, T., and Schulz, M.: NCC NorESM2-MM model output prepared for CMIP6 CMIP piControl, https://doi.org/10.22033/ESGF/CMIP6.8221, 2019.

Bethke, I., Wang, Y., Counillon, F., Kimmritz, M., Fransner, F., Samuelsen, A., Langehaug, H. R., Chiu, P.-G., Bentsen, M., Guo, C., Tjiputra, J., Kirkevåg, A., Oliviè, D. J. L., Seland, O., Fan, Y., Lawrence, P., Eldevik, T., and Keenlyside, N.: NCC NorCPM1 model output prepared for CMIP6 CMIP piControl, https://doi.org/10.22033/esgf/cmip6.10896, 2019.

Boucher, O., Denvil, S., Levavasseur, G., Cozic, A., Caubel, A., Foujols, M.-A., Meurdesoif, Y., Cadule, P., Devilliers, M., Ghattas, J., Lebas, N., Lurton, T., Mellul, L., Musat, I., Mignot, J., and Cheruy, F.: IPSL IPSL-CM6A-LR model output prepared for CMIP6 CMIP piControl, https://doi.org/10.22033/ESGF/CMIP6.5251, 2018.

Boucher, O., Denvil, S., Levavasseur, G., Caubel, A., Cozic, A., Foujols, M.-A., Meurdesoif, Y., Cadule, P., Devilliers, M., Ghattas, J., Lebas, N., Lurton, T., Mellul, L., Musat, I., Mignot, J., and Cheruy, F.: IPSL IPSL-CM6A-MR1 model output prepared for CMIP6 CMIP piControl, https://doi.org/10.22033/esgf/cmip6.15944, 2023.

Cao, J. and Wang, B.: NUIST NESMv3 model output prepared for CMIP6 CMIP piControl, https://doi.org/10.22033/ESGF/CMIP6.8776, 2019.

Chai, Z.: CAS CAS-ESM1.0 model output prepared for CMIP6 CMIP piControl, https://doi.org/10.22033/esgf/cmip6.3445, 2020.

Danabasoglu, G.: NCAR CESM2-FV2 model output prepared for CMIP6 CMIP piControl, https://doi.org/10.22033/ESGF/CMIP6.11301, 2019a.

Danabasoglu, G.: NCAR CESM2-WACCM-FV2 model output prepared for CMIP6 CMIP piControl, https://doi.org/10.22033/ESGF/CMIP6.11302, 2019b.

Danabasoglu, G.: NCAR CESM2-WACCM model output prepared for CMIP6 CMIP piControl, https://doi.org/10.22033/ESGF/CMIP6.10094, 2019c.

Danabasoglu, G., Lawrence, D., Lindsay, K., Lipscomb, W., and Strand, G.: NCAR CESM2 model output prepared for CMIP6 CMIP piControl, https://doi.org/10.22033/ESGF/CMIP6.7733, 2019.

Dix, M., Bi, D., Dobrohotoff, P., Fiedler, R., Harman, I., Law, R., Mackallah, C., Marsland, S., O'Farrell, S., Rashid, H., Srbinovsky, J., Sullivan, A., Trenham, C., Vohralik, P., Watterson, I., Williams, G., Woodhouse, M., Bodman, R., Dias, F. B., Domingues, C. M., Hannah, N., Heerdegen, A., Savita, A., Wales, S., Allen, C., Druken, K., Evans, B., Richards, C., Ridzwan, S. M., Roberts, D., Smillie, J., Snow, K., Ward, M., and Yang, R.: CSIRO-ARCCSS ACCESS-CM2 model output prepared for CMIP6 CMIP piControl, https://doi.org/10.22033/ESGF/CMIP6.4311, 2019.

EC-Earth Consortium (EC-Earth): EC-Earth-Consortium EC-Earth3-Veg model output prepared for CMIP6 CMIP piControl, https://doi.org/10.22033/ESGF/CMIP6.4848, 2019a.

EC-Earth Consortium (EC-Earth): EC-Earth-Consortium EC-Earth3 model output prepared for CMIP6 CMIP piControl, https://doi.org/10.22033/ESGF/CMIP6.4842, 2019b.

EC-Earth Consortium (EC-Earth): EC-Earth-Consortium EC-Earth3-LR model output prepared for CMIP6 CMIP piControl, https://doi.org/10.22033/esgf/cmip6.4847, 2019c.

EC-Earth Consortium (EC-Earth): EC-Earth-Consortium EC-Earth3-AerChem model output prepared for CMIP6 CMIP piControl, https://doi.org/10.22033/ESGF/CMIP6.4843, 2020a.

EC-Earth Consortium (EC-Earth): EC-Earth-Consortium EC-Earth3-Veg-LR model output prepared for CMIP6 CMIP piControl, https://doi.org/10.22033/ESGF/CMIP6.4849, 2020b.

EC-Earth Consortium (EC-Earth): EC-Earth-Consortium EC-Earth-3-CC model output prepared for CMIP6 CMIP piControl, https://doi.org/10.22033/ESGF/CMIP6.4844, 2021.

Jungclaus, J., Bittner, M., Wieners, K.-H., Wachsmann, F., Schupfner, M., Legutke, S., Giorgetta, M., Reick, C., Gayler, V., Haak, H., Vrese, P. d., Raddatz, T., Esch, M., Mauritsen, T., Storch, J.-S. v., Behrens, J., Brovkin, V., Claussen, M., Crueger, T., Fast, I., Fiedler, S., Hagemann, S., Hohenegger, C., Jahns, T., Kloster, S., Kinne, S., Lasslop, G., Kornblueh, L., Marotzke, J., Matei, D., Meraner, K., Mikolajewicz, U., Modali, K., Müller, W., Nabel, J., Notz, D., Gehlen, K. P.-v., Pincus, R., Pohlmann, H., Pongratz, J., Rast, S., Schmidt, H., Schnur, R., Schulzweida, U., Six, K., Stevens, B., Voigt, A., and Roeckner, E.: MPI-M MPI-ESM1.2-HR model output prepared for CMIP6 CMIP piControl, https://doi.org/10.22033/ESGF/CMIP6.6674, 2019.

Kim, Y., Noh, Y., Kim, D., Lee, M.-I., Lee, H. J., Kim, S. Y., and Kim, D.: KIOST KIOST-ESM model output prepared for CMIP6 CMIP piControl, https://doi.org/10.22033/esgf/cmip6.5303, 2019.

Krasting, J. P., John, J. G., Blanton, C., McHugh, C., Nikonov, S., Radhakrishnan, A., Rand, K., Zadeh, N. T., Balaji, V., Durachta, J., Dupuis, C., Menzel, R., Robinson, T., Underwood, S., Vahlenkamp, H., Dunne, K. A., Gauthier, P. P., Ginoux, P., Griffies, S. M., Hallberg, R., Harrison, M., Hurlin, W., Malyshev, S., Naik, V., Paulot, F., Paynter, D. J., Ploshay, J., Reichl, B. G., Schwarzkopf, D. M., Seman, C. J., Silvers, L., Wyman, B., Zeng, Y., Adcroft, A., Dunne, J. P., Dussin, R., Guo, H., He, J., Held, I. M., Horowitz, L. W., Lin, P., Milly, P., Shevliakova, E., Stock, C., Winton, M., Wittenberg, A. T., Xie, Y., and Zhao, M.: NOAA-GFDL GFDL-ESM4 model output prepared for CMIP6 CMIP piControl, https://doi.org/10.22033/esgf/cmip6.8669, 2018.

Li, L.: CAS FGOALS-g3 model output prepared for CMIP6 CMIP piControl, https://doi.org/10.22033/ESGF/CMIP6.3448, 2019.

Lorenz, S., Jungclaus, J., Schmidt, H., Haak, H., Reick, C., Schupfner, M., Wachsmann, F., Gayler, V., Vrese, P. d., Raddatz, T., Mauritsen, T., Storch, J.-S. v., Brovkin, V., Claussen, M., Crueger, T., Fiedler, S., Hagemann, S., Hohenegger, C., Jahns, T., Kinne, S., Kornblueh, L., Marotzke, J., Mikolajewicz, U., Modali, K., Müller, W., Nabel, J., Notz, D., Pincus, R., Pohlmann, H., Rast, S., Schnur, R., Schulzweida, U., Six, K., Stevens, B., Roeckner, E., Wieners, K.-H., Esch, M., Giorgetta, M., and Ilyina, T.: MPI-M ICON-ESM-LR model output prepared for CMIP6 CMIP piControl, https://doi.org/10.22033/esgf/cmip6.6673, 2021.

Lovato, T. and Peano, D.: CMCC CMCC-CM2-SR5 model output prepared for CMIP6 CMIP piControl, https://doi.org/10.22033/ESGF/CMIP6.3874, 2020.

Lovato, T., Peano, D., and Butenschön, M.: CMCC CMCC-ESM2 model output prepared for CMIP6 CMIP piControl, https://doi.org/10.22033/ESGF/CMIP6.13241, 2021.

Mulcahy, J., Rumbold, S., Tang, Y., Walton, J., Hardacre, C., Stringer, M., Hill, R., Kuhlbrodt, T., and Jones, C.: MOHC UKESM1.1-LL model output prepared for CMIP6 CMIP piControl, https://doi.org/10.22033/ESGF/CMIP6.16823, 2022.

NASA Goddard Institute for Space Studies (NASA/GISS): NASA-GISS GISS-E2.1G model output prepared for CMIP6 CMIP piControl, https://doi.org/10.22033/ESGF/CMIP6.7380, 2018.

NASA Goddard Institute for Space Studies (NASA/GISS): NASA-GISS GISS-E2-2-G model output prepared for CMIP6 CMIP piControl, https://doi.org/10.22033/ESGF/CMIP6.7382, 2019.

Neubauer, D., Ferrachat, S., Drian, C. S.-L., Stoll, J., Folini, D. S., Tegen, I., Wieners, K.-H., Mauritsen, T., Stemmler, I., Barthel, S., Bey, I., Daskalakis, N., Heinold, B., Kokkola, H., Partridge, D., Rast, S., Schmidt, H., Schutgens, N., Stanelle, T., Stier, P., Watson-Parris, D., and Lohmann, U.: HAMMOZ-Consortium MPI-ESM1.2-HAM model output prepared for CMIP6 CMIP piControl, https://doi.org/10.22033/ESGF/CMIP6.5037, 2019.

Ridley, J., Menary, M., Kuhlbrodt, T., Andrews, M., and Andrews, T.: MOHC HadGEM3-GC31-LL model output prepared for CMIP6 CMIP piControl, https://doi.org/10.22033/ESGF/CMIP6.6294, 2018.

Ridley, J., Menary, M., Kuhlbrodt, T., Andrews, M., and Andrews, T.: MOHC HadGEM3-GC31-MM model output prepared for CMIP6 CMIP piControl, https://doi.org/10.22033/ESGF/CMIP6.6297, 2019.

Seferian, R.: CNRM-CERFACS CNRM-ESM2-1 model output prepared for CMIP6 CMIP piControl, https://doi.org/10.22033/esgf/cmip6.4165, 2018.

Seland, O., Bentsen, M., Oliviè, D. J. L., Toniazzo, T., Gjermundsen, A., Graff, L. S., Debernard, J. B., Gupta, A. K., He, Y., Kirkevåg, A., Schwinger, J., Tjiputra, J., Aas, K. S., Bethke, I., Fan, Y., Griesfeller, J., Grini, A., Guo, C., Ilicak, M., Karset, I. H. H., Landgren, O. A., Liakka, J., Moseid, K. O., Nummelin, A., Spensberger, C., Tang, H., Zhang, Z., Heinze, C., Iversen, T., and Schulz, M.: NCC NorESM2-LM model output prepared for CMIP6 CMIP piControl, https://doi.org/10.22033/ESGF/CMIP6.8217, 2019.

Swart, N. C., Cole, J. N., Kharin, V. V., Lazare, M., Scinocca, J. F., Gillett, N. P., Anstey, J., Arora, V., Christian, J. R., Jiao, Y., Lee, W. G., Majaess, F., Saenko, O. A., Seiler, C., Seinen, C., Shao, A., Solheim, L., Salzen, K. v., Yang, D., Winter, B., and Sigmond, M.: CCCma CanESM5.1 model output prepared for CMIP6 CMIP piControl, https://doi.org/10.22033/ESGF/CMIP6.3673, 2019a.

Swart, N. C., Cole, J. N., Kharin, V. V., Lazare, M., Scinocca, J. F., Gillett, N. P., Anstey, J., Arora, V., Christian, J. R., Jiao, Y., Lee, W. G., Majaess, F., Saenko, O. A., Seiler, C., Seinen, C., Shao, A., Solheim, L., Salzen, K. v., Yang, D., Winter, B., Sigmond, M., Abraham, C., Akingunola, A., and Reader, C.: CCCma CanESM5.1 model output prepared for CMIP6 CMIP piControl, https://doi.org/10.22033/ESGF/CMIP6.17424, 2019b.

Tang, Y., Rumbold, S., Ellis, R., Douglas, K., Mulcahy, J., Sellar, A., Walton, J., and Jones, C.: MOHC UKESM1.0-LL model output prepared for CMIP6 CMIP piControl, https://doi.org/10.22033/ESGF/CMIP6.6298, 2019.

Tatebe, H. and Watanabe, M.: MIROC MIROC6 model output prepared for CMIP6 CMIP piControl, https://doi.org/10.22033/ESGF/CMIP6.5711, 2018.

Voldoire, A.: CMIP6 simulations of the CNRM-CERFACS based on CNRM-CM6-1 model for CMIP experiment piControl, https://doi.org/10.22033/esgf/cmip6.4163, 2018.

Voldoire, A.: CNRM-CERFACS CNRM-CM6-1-HR model output prepared for CMIP6 CMIP piControl, https://doi.org/10.22033/esgf/cmip6.4164, 2019.

Wieners, K.-H., Giorgetta, M., Jungclaus, J., Reick, C., Esch, M., Bittner, M., Legutke, S., Schupfner, M., Wachsmann, F., Gayler, V., Haak, H., Vrese, P. d., Raddatz, T., Mauritsen, T., Storch, J.-S. v., Behrens, J., Brovkin, V., Claussen, M., Crueger, T., Fast, I., Fiedler, S., Hagemann, S., Hohenegger, C., Jahns, T., Kloster, S., Kinne, S., Lasslop, G., Kornblueh, L., Marotzke, J., Matei, D., Meraner, K., Mikolajewicz, U., Modali, K., Müller, W., Nabel, J., Notz, D., Gehlen, K. P.-v., Pincus, R., Pohlmann, H., Pongratz, J., Rast, S., Schmidt, H., Schnur, R., Schulzweida, U., Six, K., Stevens, B., Voigt, A., and Erich Roeckner: MPI-M MPI-ESM1.2-LR model output prepared for CMIP6 CMIP piControl, https://doi.org/10.22033/ESGF/CMIP6.6675, 2019.

Wu, T., Chu, M., Dong, M., Fang, Y., Jie, W., Li, J., Li, W., Liu, Q., Shi, X., Xin, X., Yan, J., Zhang, F., Zhang, J., Zhang, L., and Zhang, Y.: BCC BCC-CSM2MR model output prepared for CMIP6 CMIP piControl, https://doi.org/10.22033/ESGF/CMIP6.3016, 2018.

Yu, Y.: CAS FGOALS-f3-L model output prepared for CMIP6 CMIP piControl, https://doi.org/10.22033/ESGF/CMIP6.3447, 2019.

Yukimoto, S., Koshiro, T., Kawai, H., Oshima, N., Yoshida, K., Urakawa, S., Tsujino, H., Deushi, M., Tanaka, T., Hosaka, M., Yoshimura, H., Shindo, E., Mizuta, R., Ishii, M., Obata, A., and Adachi, Y.: MRI MRI-ESM2.0 model output prepared for CMIP6 CMIP piControl, https://doi.org/10.22033/ESGF/CMIP6.6900, 2019.

Zhang, J., TongwenWu, Shi, X., Zhang, F., Li, J., Chu, M., Liu, Q., Yan, J., Ma, Q., and Wei, M.: BCC BCC-ESM1 model output prepared for CMIP6 CMIP piControl, https://doi.org/10.22033/ESGF/CMIP6.3017, 2018.

Ziehn, T., Chamberlain, M., Lenton, A., Law, R., Bodman, R., Dix, M., Wang, Y., Dobrohotoff, P., Srbinovsky, J., Stevens, L., Vohralik, P., Mackallah, C., Sullivan, A., O'Farrell, S., and Druken, K.: CSIRO ACCESS-ESM1.5 model output prepared for CMIP6 CMIP piControl, https://doi.org/10.22033/esgf/cmip6.4312, 2019.